

Axial decorated Ising model with competing interaction

This article has been downloaded from IOPscience. Please scroll down to see the full text article.

1986 J. Phys. A: Math. Gen. 19 3049

(<http://iopscience.iop.org/0305-4470/19/15/027>)

View [the table of contents for this issue](#), or go to the [journal homepage](#) for more

Download details:

IP Address: 129.252.86.83

The article was downloaded on 31/05/2010 at 19:22

Please note that [terms and conditions apply](#).

Axial decorated Ising model with competing interaction†

R J V dos Santos‡, S Coutinho§ and J R L de Almeida§

‡ Departamento de Física, Universidade Federal de Alagoas, 57.000 Maceió, Brazil

§ Departamento de Física, Universidade Federal de Pernambuco, 50.000 Recife, Brazil

Received 13 November 1985

Abstract. The phase diagram and the thermodynamics of the axial decorated Ising model on a square lattice with m -dimensional bond spins are studied for the $m = 1$ (Ising), $m = 2$ (XY), $m = 3$ (Heisenberg) and $m = \infty$ cases. Competing interactions between the site and decorating bond spins have been considered. The expressions for the partition function, the thermodynamics and the pair correlation functions of the decorated Ising chain have been analytically obtained. The effect of the dimensionality of the decorating bond spin on the thermodynamic behaviour of both models is analysed.

1. Introduction

There is currently great interest in the study of Ising systems with competing interactions. A competing interaction can be introduced, by decorating the lattice with bond spins, that simulates an effective interaction between the site Ising spins that is temperature and magnetic field dependent. For example, a class of decorated spin- $\frac{1}{2}$ Ising models has been considered by Huse *et al* (1981) in an attempt to study the axial next-nearest-neighbour Ising or ANNNI model.

This paper is devoted to the study of the phase diagram of the axial decorated Ising model on a square lattice where the decorating bond spin is a general m -dimensional vector spin with magnitude λ (see figure 1(a)). The decoration-iteration transformation has often been used to investigate the relations between the partition

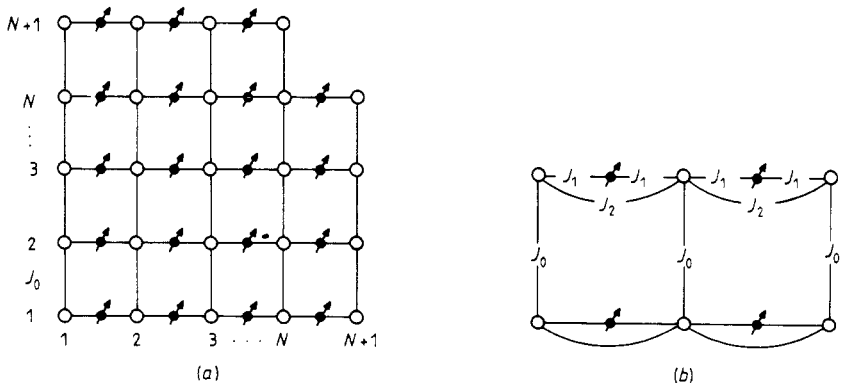


Figure 1. (a) Axial decorated Ising model on a square lattice. \circ , Ising spin σ ; \uparrow , m -dimensional decorating bond spin S . (b) Scheme of the model exchange interactions ($J_1, J_0 > 0$ and $J_2 < 0$).

† Work partially supported by CNPq, CAPES and FINEP (Brazilian agencies).

functions for distinct lattice models. We refer to Syozi (1972) as a general reference. Several plane Ising lattices decorated with higher Ising spins have been studied by Yamada (1969) pointing out the existence of three phase-transition temperatures in both isotropic and axially decorated square lattice models. By higher Ising spins Yamada (1969) means a spin variable that can take $l(l > 2)$ discrete values. In the present model the decorating spin is a m -dimensional vector spin varying continuously that reduces to particular cases for $m = 1$ (Ising), $m = 2$ (XY) and $m = 3$ (Heisenberg). The isotropic version of the Ising model on a square lattice with the present kind of decoration has recently been considered by Horiguchi and Gonçalves (1983) showing the possibility of the existence of three phase-transition temperatures for $m > 1$. In the present paper we consider the anisotropic or axial decorated Ising model on a square lattice which has three phase-transition temperatures even for $m = 1$ and can be considered the simplest version of the ANNNI mock model generalised for vector spins. This model for the particular case $m = 1$ has already been studied by Yamada (1969) and Syozi (1968). The phase diagram shows that the range of values of the competing parameters for the existence of the three phase-transition point increases with the increase of the dimensionality m of the decorating spin. We also study the effect of the dimensionality of the decorating spin on the critical behaviour of the system especially in the limiting case where $m \rightarrow \infty$.

Our square lattice model can be regarded as a set of linear decorated Ising chains (rows) interacting with their first neighbour's chains through a ferromagnetic exchange interaction (constant coupling $J_0 > 0$). Within each chain the nearest-neighbour Ising site spins couple through an antiferromagnetic exchange interaction (coupling constant $J_2 < 0$) while interacting with the vector bond spins through a ferromagnetic interaction (coupling constant $J_1 > 0$). A sketch of these interactions is shown in figure 1(b).

As the bond vector spins do not interact with each other they can be traced out in the partition function yielding a temperature dependent effective ferromagnetic interaction between the Ising site spins competing with the antiferromagnetic one. Actually our model is equivalent to an anisotropic square lattice Ising model with a temperature dependent effective interaction in the decorated direction and a constant ferromagnetic interaction in the off-decorated direction.

In § 2 we review the thermodynamic and magnetic properties of an Ising chain decorated with m -dimensional vector spins under an external magnetic field by evaluating exactly the analytic partition function, the effective interaction, the correlation functions and the thermodynamic functions (internal energy, entropy and specific heat).

In § 3 we present the axial decorated Ising model on a square lattice and discuss its phase diagram in the T against $\alpha = (-J_2/\lambda J_1)$ plane whereas the phase transition lines $\alpha_c(T_c)$ are calculated exactly and explicitly. The specific heat and internal energy are also exactly calculated and shown as functions of the temperature for several values of m and α . It is shown that within the range of values of α for which the phase diagram has three transition temperatures there appears an apparent first-order phase transition evidenced by a jump in the specific heat.

In § 4 we study both one- and two-dimensional models in the limit where the dimensionality of the decorated spins goes to infinity. Finally in § 5 we summarise our work by presenting our conclusions.

2. Decorated Ising chain

We consider an Ising chain of N spins σ decorated with $(N - 1)$ m -dimensional vector bond spins with free boundary conditions and submitted to an external uniform magnetic

field H . The Ising spins interact with the vector bond spins through a ferromagnetic interaction (coupling constant $J_1 > 0$) and with the nearest-neighbour Ising site spins through an antiferromagnetic interaction (coupling constant $J_2 < 0$). The vector bond spins do not interact with each other.

The Hamiltonian of the system is then

$$H = -J_1 \sum_{i=1}^{N-1} S_i^1 (\sigma_i + \sigma_{i-1}) - J_2 \sum_{i=1}^{N-1} \sigma_i \sigma_{i+1} - H \sum_{i=1}^N \sigma_i - H \sum_{i=1}^{N-1} S_i^1 \tag{1}$$

where $S_i^\nu (\nu = 1, 2, \dots, m)$ are the cartesian components of the m -dimensional vector spin S_i of magnitude λ , and H is applied in the $\nu = 1$ direction.

2.1. The partition function and effective interaction

The normalised partition function for the Hamiltonian H is given by

$$Z_N(m) = \sum_{\{\sigma\}} \int \{dS\} \exp(-\beta H) \left(\int \{dS\} \right)^{-1} \tag{2}$$

where the summation is taken over all the Ising spin configurations, $\beta = (K_B T)^{-1}$ and

$$\int \{dS\} \Phi\{S\} = \int \prod_{i=1}^{N-1} dS \delta(\lambda^2 - S_i^2) \Phi\{S\}. \tag{3}$$

Taking $\Phi\{S\} = 1$ we get for the denominator of (2),

$$\int d\{S\} = \left(\frac{\pi^{m/2} \lambda^{m-2}}{\Gamma(\frac{1}{2}m)} \right)^{N-1} \tag{4}$$

where $\Gamma(x)$ is the gamma function.

To evaluate the trace in the vector bond spin variables we use the approach of Stanley (1969) obtaining

$$Z_N(m) = \Lambda_n^{N-1} (1 + \delta_{1,m})^{N-1} \sum_{\sigma_1, \sigma_N} \langle \sigma_1 | [\exp(\frac{1}{2}K\sigma_1) \mathbf{T}^{N-1} \exp(\frac{1}{2}K\sigma_N)] | \sigma_N \rangle \tag{5}$$

where

$$\Lambda_n = 2^n \Gamma(n+1) \tag{6}$$

$n = (m/2) - 1$, $\delta_{1,m}$ is the Kronecker delta function and \mathbf{T} is the transfer matrix whose matrix elements are given by

$$\langle \sigma | \mathbf{T} | \sigma' \rangle = \psi_n(\sigma, \sigma') \exp[K_2 \sigma \sigma' + \frac{1}{2}K(\sigma + \sigma')] \tag{7}$$

where

$$\psi_n(\sigma, \sigma') = u^{-n} I_n(u) \tag{8}$$

$I_n(u)$ being the modified Bessel function of the first kind of order n , $u = \lambda K_1(\sigma + \sigma' + K/K_1)$, $K_1 = \beta J_1$, $K_2 = \beta J_2$ and $K = \beta H$.

We make use of the decoration-iteration (Fisher 1959) for the transfer matrix to obtain

$$\langle \sigma | \mathbf{T} | \sigma' \rangle = f \exp[K_{\text{eff}} \sigma \sigma' + \frac{1}{2}L(\sigma + \sigma')] \tag{9}$$

where

$$K_{\text{eff}} = K_2 + \frac{1}{4} \ln \frac{\psi_n(1, 1)\psi_n(-1, -1)}{\psi_n^2(-1, 1)} \tag{10}$$

$$L = K + \frac{1}{2} \ln \frac{\psi_n(1, 1)}{\psi_n(-1, -1)} \tag{11}$$

$$f = [\psi_n(1, 1)\psi_n(-1, -1)\psi_n^2(-1, 1)]^{1/4}. \tag{12}$$

Therefore, the problem is now reduced to one of obtaining the partition function of an Ising chain with an effective coupling $\beta^{-1}K_{\text{eff}}$ between spins and submitted to a modified magnetic field $\beta^{-1}L$ acting on all the spins, except on the border ones where the field is actually $\beta^{-1}[L - \ln \psi_n(1, 1)/\psi_n(-1, -1)]$ in the case of free ends chain. Moreover the effective coupling and the modified magnetic field are both temperature and magnetic field dependent through the functions $\psi_n(\sigma, \sigma')$.

After straightforward calculations we obtain the partition function for the free ends chain, that is

$$Z_N(m) = \Lambda_n^{N-1} \lambda_+^{N-1} (1 + \delta_{1,m})^{N-1} [A_+ + A_-(\lambda_-/\lambda_+)^{N-1}] \tag{13}$$

where λ_{\pm} are the transfer matrix eigenvalues given by

$$\lambda_{\pm} = f \exp(K_{\text{eff}}) \{ \cosh L \pm [\sinh^2 L + \exp(-4K_{\text{eff}})]^{1/2} \} \tag{14}$$

and

$$A_{\pm} = [\cosh K \pm (1 - \Delta)^{1/2} \sinh K \pm \Delta^{1/2}] \tag{15}$$

$$\Delta = [1 + \exp(4K_{\text{eff}}) \sinh^2 L]^{-1}. \tag{16}$$

In the $H \rightarrow 0$ limit the partition function reduces to the simple expression

$$Z_N^0(m) = 2(1 + \delta_{1,m})^{N-1} \left(\Lambda_n \frac{I_n(2\lambda K_1)}{(2\lambda K_1)^n} \exp(K_2) + \exp(-K_2) \right)^{N-1}. \tag{17}$$

2.2. Correlation functions

In this subsection we obtain the exact expressions for the correlation functions $\langle \sigma_k \sigma_l \rangle$, $\langle \mathbf{S}_k \cdot \mathbf{S}_l \rangle$ and $\langle \sigma_k S_l^1 \rangle$, respectively the site-site, the bond-bond and the site-bond spin correlation functions.

The site-site spin correlation function $\langle \sigma_k \sigma_l \rangle$ can be easily obtained from

$$\begin{aligned} \langle \sigma_k \sigma_l \rangle &= \frac{\Lambda_n^{N-1} (1 + \delta_{1,m})^{N-1}}{Z_N(m)} \sum_{\sigma_1 \sigma_k \sigma_N} \langle \sigma_1 | \exp(\frac{1}{2} K \sigma_1) \mathbf{T}^{k-1} | \sigma_k \rangle \\ &\quad \times \langle \sigma_k | \sigma_k \mathbf{T}^{l-k} | \sigma_l \rangle \langle \sigma_l | \sigma_l \mathbf{T}^{n-l} \exp(\frac{1}{2} K \sigma_N) | \sigma_N \rangle. \end{aligned} \tag{18}$$

The general expression for this correlation function in the case of a free ends chain can be obtained straightforwardly giving an enormous expression†. We limit ourselves to the bulk limit, i.e. the limit where the two spins to be correlated are at a finite distance from each other but infinitely far from the boundary. In this limit the correlation function for the free ends chain equals the one for the ring chain, i.e.

$$\langle \sigma_k \sigma_l \rangle = 1 + \Delta [(\lambda_-/\lambda_+)^{l-k} - 1]. \tag{19}$$

† See, for example, McCoy and Wu (1973, p 42).

The zero-field correlation function ($\Delta = 1$) is

$$\langle \sigma_k \sigma_l \rangle^0 = (\tanh K_{\text{eff}}^0)^{|l-k|} \tag{20}$$

where

$$K_{\text{eff}}^0 = K_2 + \frac{1}{2} \ln[\psi_n(1, 1)/\psi_n(-1, 1)]. \tag{21}$$

The bond-bond correlation function $\langle \mathbf{S}_k \cdot \mathbf{S}_l \rangle$ can be evaluated from

$$\langle \mathbf{S}_k \cdot \mathbf{S}_l \rangle = (1 + \delta_{l,m})^{N-1} \sum_{\{\sigma\}} \int \{d\mathbf{S}\} \mathbf{S}_k \cdot \mathbf{S}_l \exp(-\beta H) \left(Z_N(m) \int \{d\mathbf{S}\} \right)^{-1}. \tag{21'}$$

Tracing out the vector bond spin variables one obtains

$$\langle \mathbf{S}_k \cdot \mathbf{S}_l \rangle = \frac{\lambda^2 \Lambda_n^{N-1} (1 + \delta_{l,m})^{N-1}}{Z_N(m)} \sum_{\sigma, \sigma_N} \langle \sigma_1 | \exp(\frac{1}{2} K \sigma_1) \mathbf{T}^{k-1} \tilde{\mathbf{T}} \mathbf{T}^{l-k-1} \tilde{\mathbf{T}} \mathbf{T}^{N-l-1} \exp(\frac{1}{2} K \sigma_N) | \sigma_N \rangle \tag{22}$$

where

$$\langle \sigma | \tilde{\mathbf{T}} | \sigma' \rangle = u \psi_{n+1}(\sigma, \sigma') \exp[K_2 \sigma \sigma' + \frac{1}{2} K (\sigma + \sigma')]. \tag{23}$$

By using the transformation mentioned above (see (9)-(12)) one obtains for the bulk limit that

$$\langle \mathbf{S}_k \cdot \mathbf{S}_l \rangle = \left(\frac{\lambda \tilde{\lambda}_+}{4 \lambda_+} \right)^2 \left[B_+ B_- \left(\frac{\lambda_-}{\lambda_+} \right)^{l-k-1} \left(1 - \frac{\tilde{\lambda}_-}{\tilde{\lambda}_+} \right)^2 + \left(B_+ + B_- \frac{\tilde{\lambda}_-}{\tilde{\lambda}_+} \right)^2 \right] \tag{24}$$

where

$$B_{\pm} = 2[1 \pm \Delta \Delta_1 + (1 - \Delta)^{1/2} (1 - \Delta_1)^{1/2}] \tag{25}$$

and $\tilde{\lambda}_{\pm}$ and Δ_1 are given by (14) and (16) respectively where we replaced $\psi_n(\sigma, \sigma')$ by $u \psi_{n+1}(\sigma, \sigma')$. In the zero-field limit ($\Delta = 1, \Delta_1 = 0$), the correlation function is

$$\begin{aligned} \lambda^{-2} \langle \mathbf{S}_k \cdot \mathbf{S}_l \rangle^0 &= \left(\frac{\tilde{\lambda}_+^2}{\lambda_+ \lambda_-} \right)_0 \left(\frac{\lambda_-}{\lambda_+} \right)_0^{l-k} \\ &= \frac{F_n^2(2\lambda K_1)}{1 - \exp(-4K_{\text{eff}}^0)} \langle \sigma_k \sigma_l \rangle^0 \end{aligned} \tag{26}$$

where

$$F_n(x) = I_{n+1}(x)/I_n(x) \tag{27}$$

and $\langle \sigma_k \sigma_l \rangle^0$ is the site-site Ising correlation function given by (20).

The site-bond correlation function $\langle \sigma_k S_l^1 \rangle$ can be obtained in the same way as the previous one, i.e. from the definition

$$\langle \sigma_k S_l^1 \rangle = (1 + \delta_{l,m})^{N-1} \sum_{\{\sigma\}} \int \{d\mathbf{S}\} \sigma_k S_l^1 \exp(-\beta H) \left(Z_N(m) \int d\{S\} \right)^{-1} \tag{28}$$

and tracing out the vector bond spin variables getting

$$\begin{aligned} \langle \sigma_k S_l^1 \rangle &= \frac{\lambda \Lambda_m^{N-1} (1 + \delta_{l,m})^{N-1}}{Z_N(m)} \sum_{\sigma_1, \sigma_N} \langle \sigma_1 | \exp(\frac{1}{2} K \sigma_1) \mathbf{T}^{k-1} | \sigma_k \rangle \\ &\quad \times \langle \sigma_k | \sigma_k \mathbf{T}^{l-k} \tilde{\mathbf{T}} \mathbf{T}^{N-k} \exp(\frac{1}{2} K \sigma_N) | \sigma_N \rangle \end{aligned} \tag{29}$$

where \mathbf{T} and $\tilde{\mathbf{T}}$ are given by (7) and (23) respectively.

In the bulk limit this correlation function is

$$\lambda^{-1} \langle \sigma_k S_l^1 \rangle = \frac{1}{4} \left(\frac{\tilde{\lambda}_+}{\tilde{\lambda}_-} \right) \left[(\Delta B_+ B_-)^{1/2} \left(\frac{\lambda_-}{\lambda_+} \right)^{l-k} \left(\frac{\tilde{\lambda}_-}{\tilde{\lambda}_+} - 1 \right) + 2(1-\Delta)^{1/2} \left(B_+ + B_- \frac{\tilde{\lambda}_-}{\tilde{\lambda}_+} \right) \right] \quad (30)$$

and in the zero-field limit ($\Delta = 1, \Delta_1 = 0$) it reduces to

$$\lambda^{-1} \langle \sigma_k S_l^1 \rangle^0 = \left(\frac{\tilde{\lambda}_+}{\lambda_+} \right)_0 \left(\frac{\lambda_-}{\lambda_+} \right)_0^{l-k} = \frac{F_n(2\lambda K_1)}{1 + \exp(-2K_{\text{eff}}^0)} \langle \sigma_k \sigma_l \rangle^0. \quad (31)$$

The site-site correlation function $\langle \sigma_k \sigma_l \rangle^0 = 1$ when $T = 0$ and for $T \neq 0$ and $(l - k) \rightarrow \infty$ we get $\langle \sigma_k \sigma_l \rangle^0 \rightarrow 0$ for all values of the spin dimensionality, as expected for one-dimensional models. Nevertheless both the site-bond $\langle \sigma_k S_l^1 \rangle^0$ and the bond-bond $\langle \mathbf{S}_k \cdot \mathbf{S}_l \rangle^0$ are zero for $T = 0$ and $\alpha > 1$, α being the competing parameter† $\alpha = -J_2/\lambda J_1$. Therefore at $T = 0$ and for strong antiferromagnetic interaction J_2 between the Ising spins, the decorating vector spins remain uncorrelated while the Ising spins are ordered antiferromagnetically. On the other hand, for $\alpha < 1$ the ground-state configuration shows that both Ising and vector spin systems are ordered ferromagnetically.

The short-range order can be analysed by looking at the behaviour of the site-spin pair correlation function. In figure 2 we show the behaviour of the temperature T_c , where the nearest-neighbour correlation function changes signal, against the competing parameter $\alpha = -J_2/\lambda J_1$, for three values of the spin dimensionality. We note that the ferromagnetic short-range order decreases monotonically when the decorating vector spin dimensionality increases for a given temperature, as expected (Stanley 1971).

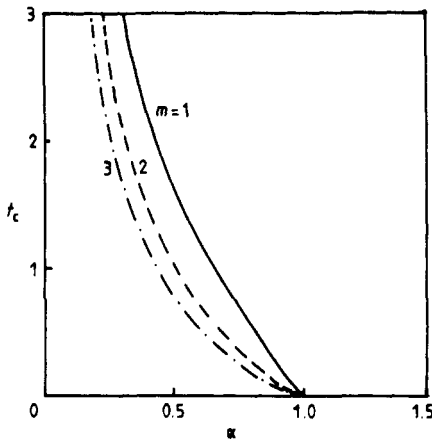


Figure 2. Short-range order behaviour. Temperature dependence of the signal changing of the pair correlation function against the competing parameter $\alpha = -J_2/\lambda J_1$ for $m = 1, 2$ and 3 (1D model).

† We have assumed that the magnitude of the vector spin λ is equal to $m^{1/2}$ in order to renormalise the exchange integrals with respect to the vector spin dimensionality (Stanley 1969).

2.3. The thermodynamic functions

The thermodynamic functions of the system can be obtained exactly from the analytical expression of the normalised free energy (free energy per spin) defined by

$$F = -K_B T \ln Z = \lim_{N \rightarrow \infty} \left(\frac{-K_B T}{(2N-1)} \ln Z_N(m) \right) = -\frac{1}{2} K_B T \ln(\Lambda_n \lambda_+) \quad (32)$$

where Λ_n and λ_+ are given by equations (6) and (14) respectively.

The internal energy $U(H, \beta)$, the entropy $S(H, \beta)$ and the specific heat $C_H(\beta)$ can be evaluated straightforwardly from the usual thermodynamic relations $U = \partial(\beta F)/\partial\beta$, $S = K_B \beta(U - F)$ and $C_H = -K_B \beta^2 (\partial U / \partial \beta)_H$ respectively. We omit the explicit expressions of U , S and C_H for the non-zero magnetic field case because they are too large for analytical purposes. Nevertheless, in the zero-field case we have

$$U = \frac{1}{2} J_2 - [1 + \exp(-2K_{\text{eff}}^0)]^{-1} K'_{\text{eff}} \quad (33)$$

$$S / K_B = \frac{1}{2} \ln[1 + \exp(2K_{\text{eff}}^0)] - \beta K'_{\text{eff}} [1 + \exp(-2K_{\text{eff}}^0)]^{-1} + \frac{1}{2} \delta_{1,m} \ln 2 \quad (34)$$

$$C / K_B = \beta^2 \{ K''_{\text{eff}} + 2(K'_{\text{eff}})^2 [1 + \exp(2K_{\text{eff}}^0)]^{-1} \} [1 + \exp(-2K_{\text{eff}}^0)]^{-1} \quad (35)$$

where

$$K_{\text{eff}}^0 = \beta J_2 + \frac{1}{2} \ln G_n(2\lambda K_1) \quad (36)$$

$$K'_{\text{eff}} = \partial K_{\text{eff}}^0 / \partial \beta = J_2 + \lambda J_1 F_n(2\lambda K_1) \quad (37)$$

$$K''_{\text{eff}} = \partial^2 K_{\text{eff}}^0 / \partial \beta^2 = 2(\lambda J_1)^2 \left(1 - \frac{2n+1}{2\lambda K_1} F_n(2\lambda K_1) - F_n^2(2\lambda K_1) \right) \quad (38)$$

$$G_n(x) = 2^n \Gamma(n+1) x^{-n} I_n(x) \quad (39)$$

and $F_n(x)$ is given by (27).

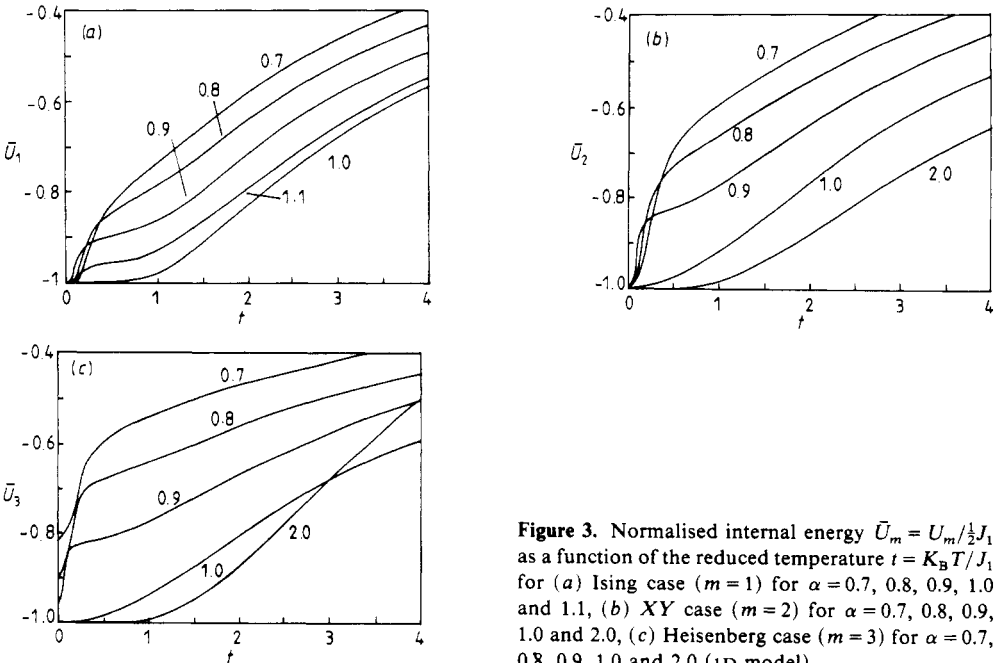


Figure 3. Normalised internal energy $\bar{U}_m = U_m / \frac{1}{2} J_1$ as a function of the reduced temperature $t = K_B T / J_1$ for (a) Ising case ($m=1$) for $\alpha = 0.7, 0.8, 0.9, 1.0$ and 1.1 , (b) XY case ($m=2$) for $\alpha = 0.7, 0.8, 0.9, 1.0$ and 2.0 , (c) Heisenberg case ($m=3$) for $\alpha = 0.7, 0.8, 0.9, 1.0$ and 2.0 (1D model).

The temperature dependence of the normalised internal energy \tilde{U} is indicated in figure 3 for several values of the competing parameter α and for each case where the decorating vector spins are Ising ($m = 1$), planar ($m = 2$) or Heisenberg ($m = 3$) spins. In the low-temperature limit we notice a qualitative interesting behaviour of the internal energy patterns: an abrupt increase from the ground-state value for $\alpha < 1$ produced by the onset of the correlation between the decorating vector spins and the Ising spins. For $\alpha > 1$ and $T \rightarrow 0$ K the vector spins remain uncorrelated as mentioned above.

The temperature behaviour of the entropy per spin is shown in figure 4. Figure 4(a) shows the Ising case unnormalised entropy for $\alpha = 0$ (pure ferromagnetic Ising chain) and $\alpha = 0.8, 1.0$ and 1.2 . For $\alpha < 1$, $S_1/K_B = 0$ at $T = 0$ as expected. However for $\alpha > 1$ the entropy has a non-zero constant value at $T = 0$. For $\alpha = 1$, $S_1/K_B = \frac{1}{2} \ln 3$ corresponding to the threefold degeneracy of the ground state when $J_1 = |J_2|$. For $\alpha > 1$, $S_1/K_B = \frac{1}{2} \ln 2$ since the decorated spins are not correlated with the site spins as pointed out in § 2.2. Figures 4(b) and 4(c) show the $m = 2$ and 3 cases respectively. Note that for $m > 1$ the entropy diverges logarithmically to $-\infty$ at low temperatures for $\alpha < 1$, diverging faster the larger m is since the 'classical' decorating bond spins are correlated with the Ising system. On the other hand, for $\alpha > 1$ and $T = 0$ the bond vector spins are not correlated and the entropy is the one for the Ising system only, since we have normalised the partition function with respect to the classical spin degrees of freedom.

In figure 5 we present the specific heat at zero field for the cases $m = 1, 2$ and 3 and for several values of the competing parameter α . For the Ising case ($m = 1$) and for $\alpha \sim 1$ the specific heat shows two maxima, a sharp one at low temperature that collapses at $T \rightarrow 0$ when $\alpha \rightarrow 1$ and a broad one that is smoothly dependent on α . The sharp maximum is associated with the short-range ferromagnetic order induced by the decorating bond spins while the broad one is due to the direct antiferromagnetic Ising coupling. For $m > 2$ cases the two maxima behaviour occurs only for $\alpha < 1$, since the

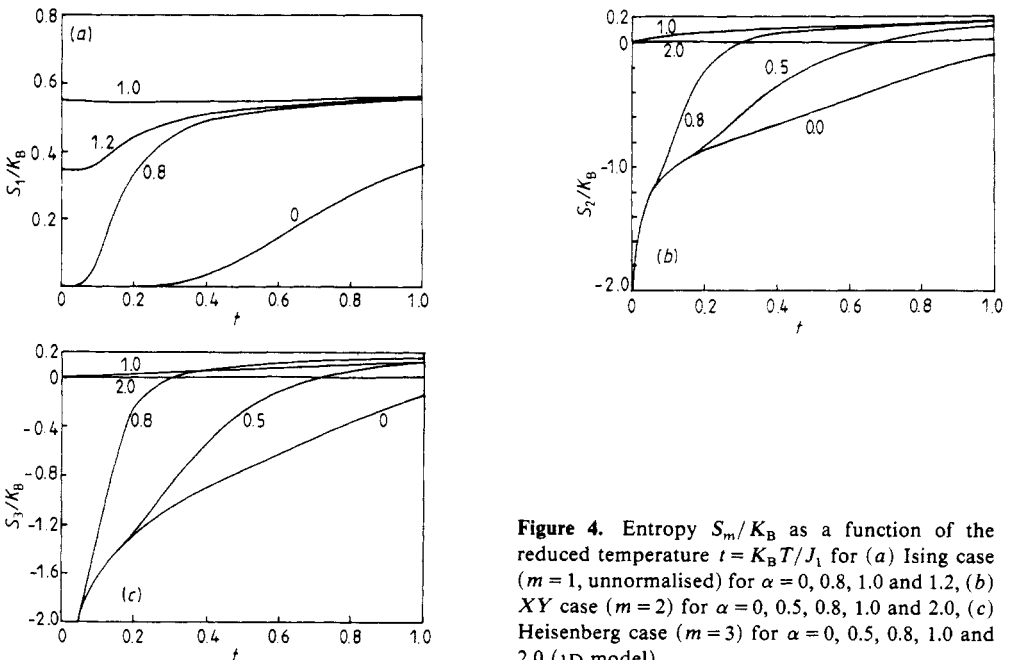


Figure 4. Entropy S_m/K_B as a function of the reduced temperature $t = K_B T / J_1$ for (a) Ising case ($m = 1$, unnormalised) for $\alpha = 0, 0.8, 1.0$ and 1.2 , (b) XY case ($m = 2$) for $\alpha = 0, 0.5, 0.8, 1.0$ and 2.0 , (c) Heisenberg case ($m = 3$) for $\alpha = 0, 0.5, 0.8, 1.0$ and 2.0 (1D model).

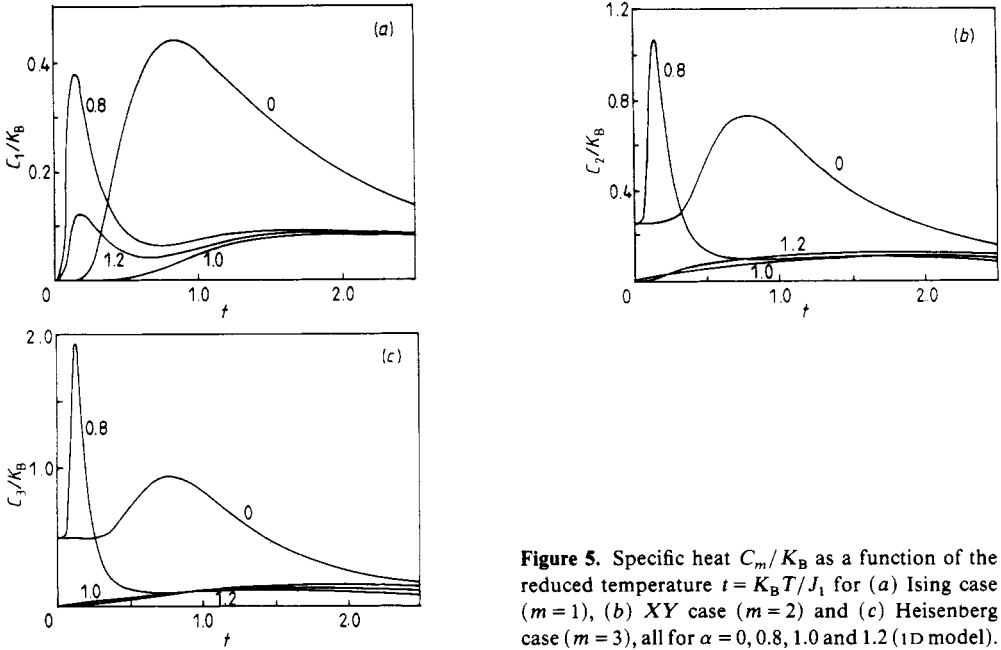


Figure 5. Specific heat C_m/K_B as a function of the reduced temperature $t = K_B T/J_1$ for (a) Ising case ($m = 1$), (b) XY case ($m = 2$) and (c) Heisenberg case ($m = 3$), all for $\alpha = 0, 0.8, 1.0$ and 1.2 (1D model).

bond spin becomes more loosely correlated as a consequence of its higher dimensionality. Note that at $T=0$, C/K_B goes at $(2n+1)/4$ due to the classical nature of the decorating bond-vector spins. As in the Ising case the sharp maximum collapses at $T \rightarrow 0$ when $\alpha \rightarrow 1$, for $m = 2, 3, \dots$, cases.

3. Axial decorated Ising model on a square lattice

In this section we extend the decorated chain model discussed in the previous section to the case of an Ising model on a square lattice decorated with m -dimensional vector spins in one direction (axial decoration) as indicated in figure 1(a). We assume toroidal boundary conditions.

The Hamiltonian of this model can be written as

$$H = -J_1 \sum_{ij} S_j^{i1} (\sigma_j^i + \sigma_{j+1}^i) - J_2 \sum_{ij} \sigma_j^i \sigma_{j+1}^i - J_0 \sum_{ij} \sigma_j^i \sigma_j^{i+1} \tag{40}$$

where J_0 , J_1 and J_2 are the interaction coupling constants as indicated in figure 1(b), σ_j^i denotes the Ising spin variables of the j th column and i th row site and $S_j^{i\gamma}$ label the γ th cartesian component of the vector bond spin at the i th bond of the j th column.

3.1. The partition function

The normalised partition function of this model can be partially evaluated by tracing out the vector spin variables and using the decoration-iteration transformation indicated in § 2. It follows that

$$Z_{N^2}(m) = \sum_{\{\sigma\}} f_n^{N^2} \exp\left(K_{\text{eff}}^0 \sum_{ij} \sigma_j^i \sigma_{j+1}^i + K_0 \sum_{ij} \sigma_j^i \sigma_j^{i+1}\right) \tag{41}$$

where $K_0 = \beta J_0$, K_{eff}^0 is given by (36) and

$$f_n = \left(\frac{I_n(2\lambda K_1)}{2^n n! (2\lambda K_1)^n} \right)^{1/2} \quad n = (m/2) - 1. \tag{42}$$

The partition function given by (41) is the Onsager partition function (see, for example, McCoy and Wu 1973) multiplied by the factor $f_n^{N^2}$. Note that f_n is temperature dependent through $K_1 = \beta J_1$. Therefore the free energy per spin variable has an extra term equal to $\ln f_n(T)$. Nevertheless the transition temperatures are not affected since $f_n(T)$ is an analytical function of T . Therefore the transition temperatures are given by the solutions of the well known transcendental equation

$$\sinh(2K_{\text{eff}}^0) \sinh(2K_0) = \pm 1. \tag{43}$$

The phase diagram in the plane $T \times \alpha$, α being the competing parameter $-J_2/\lambda J_1$, can be obtained analytically from (43), i.e.

$$\alpha = \frac{1}{x} \ln \left(\frac{G_n(x) (\cosh(\delta x) \pm 1)}{\sinh(\delta x)} \right) \tag{44}$$

where $x = 2\lambda J_1 / K_B T$, $\delta = J_0 / \lambda J_1$ and $G_n(x)$ is given by (39). In figure 6 we illustrate the phase boundaries of the present model in the $T-\alpha$ diagram, for the particular case when $\delta = 1$ and for Ising ($m = 1$), XY ($m = 2$) and Heisenberg ($m = 3$) decorating spins. For all vector spin dimensionalities the system has three phases meeting at the point $T = 0$, $\alpha = 1$: the ferromagnetic, the paramagnetic and the mixed phase (parametamagnetic). In the ferromagnetic phase both Ising and vector spins are correlated ferromagnetically. In the mixed phase the Ising spins are correlated antiferromagnetically while the bond vector spins are uncorrelated. Therefore the mixed para-metamagnetic phase at $T = 0$ ($\alpha \rightarrow 1$) can be described as a sequence of up and down ($\uparrow\downarrow\uparrow\downarrow\uparrow\downarrow\dots$) columns of Ising spins (metamagnetic) while the bond vector spins are uncorrelated (paramagnetic). In that case the ground state is infinitely degenerated. For $\alpha \leq 1$ there is a three phase-transition region that increases with the vector spin dimensionality m , for all values of m . The phase diagram of the isotropic decorated model is shown in

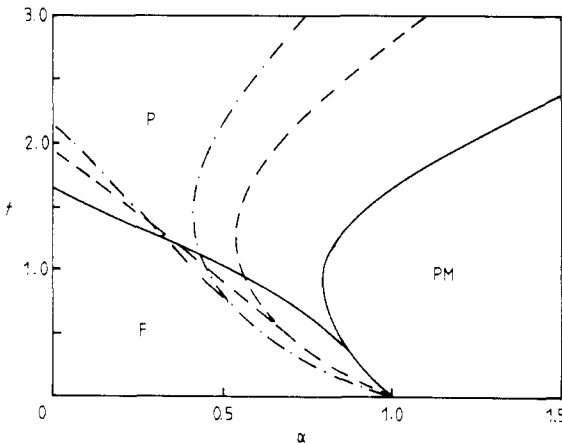


Figure 6. Phase diagram in the plane $T \times \alpha$ for the anisotropic decorated square lattice Ising model for the $m = 1$ (—), $m = 2$ (---) and $m = 3$ (- · -) cases.

figure 7. This phase diagram can easily be obtained by solving the transcendental equation $\sinh^2(2K_{\text{eff}}^0) = 1$. It shows the same features of the diagram of the present model except for the Ising type decoration ($m = 1$) in which there is no three phase-transition temperature region as obtained by other authors (Yamada 1969, Horiguchi and Gonçalves 1983). Both models have the same critical exponents of the two-dimensional Ising model. However for $\alpha \leq 1$ and as m increases the borderlines between the paramagnetic and the ferromagnetic phases and the paramagnetic and the mixed phases seems to collapse to an apparent first-order transition line. This fact is evidenced by the behaviour of the internal energy and the specific heat.

The internal energy and the specific heat can be obtained with the help of the Onsager solution (Onsager 1944). The internal energy $U(\beta)$ and the specific heat C_H are given by the usual thermodynamic relations $U = \partial(\beta F) / \partial \beta$ and $C_H = -K_B \beta^2 (\partial U / \partial \beta)_H$ respectively where F is the Helmholtz free energy per spin given by

$$F = - \lim_{N \rightarrow \infty} \frac{K_B T}{N(2N-1)} \ln Z_{N^2}(m) = -\frac{1}{2} K_B T \ln (f_n \lambda_{\text{max}}) \tag{45}$$

where λ_{max} is the largest eigenvalue of the transfer matrix of Onsager's solution for an Ising model on a square lattice with exchange interactions J_{eff}^0 and J_0 in the x and the y directions respectively.

We have from Onsager (1944) that

$$\ln \lambda_{\text{max}} = \frac{1}{2} \ln |2 \sinh(2K_0)| + \frac{1}{2\pi} \int_0^\pi \cosh^{-1} \Omega(\beta, \omega) d\omega \tag{46}$$

$\Omega(\beta, \omega)$ being given by

$$\Omega(\beta, \omega) = \cosh(2K_{\text{eff}}^0) \cosh(2K^*) - \sinh(2K_{\text{eff}}^0) \sinh(2K^*) \cos \omega \tag{47}$$

where

$$K^* = \frac{1}{2} \ln(\coth K_0). \tag{48}$$

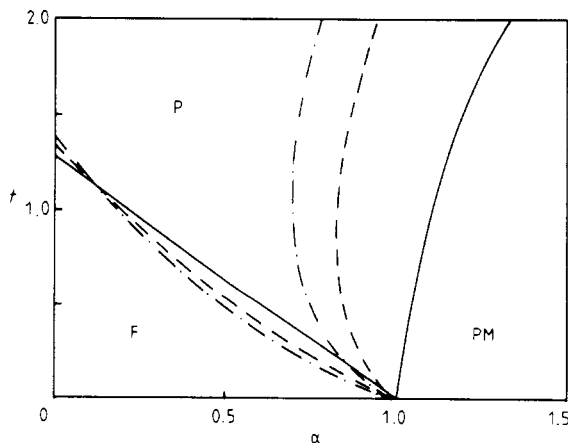


Figure 7. Phase diagram in the plane $T \times \alpha$ for the isotropic decorated square lattice Ising model for the $m = 1$ (—), $m = 2$ (---) and $m = 3$ (- · -) cases.

Therefore the internal energy and the specific heat can be evaluated straightforwardly giving

$$U = -\frac{1}{2}J_0 \coth 2K_0 - \frac{1}{2}\lambda J_1 F_n(2\lambda K_1) - \frac{1}{4\pi} \int_0^\pi \frac{\Omega'(\beta, \omega)}{[\Omega^2(\beta, \omega) - 1]^{1/2}} d\omega \tag{49}$$

$$\begin{aligned} \frac{C}{K_B} = & -K_0^2 \operatorname{cosech}^2 2K_0 + \frac{1}{2}\beta^2 K_{\text{eff}}'' \\ & + \frac{\beta^2}{4\pi} \int_0^\pi \frac{\Omega''(\beta, \omega)[\Omega^2(\beta, \omega) - 1] - \Omega(\beta, \omega)\Omega'^2(\beta, \omega)}{[\Omega^2(\beta, \omega) - 1]^{3/2}} d\omega \end{aligned} \tag{50}$$

where

$$\begin{aligned} \Omega'(\beta, \omega) = (\partial/\partial\beta)\Omega(\beta, \omega) = & 2[(K'_{\text{eff}} - K'^* \cos \omega) \sinh(2K_{\text{eff}}^0) \cosh(2K^*) \\ & + (K'^* - K'_{\text{eff}} \cos \omega) \sinh(2K^*) \cosh(2K_{\text{eff}}^0)] \end{aligned} \tag{51}$$

$$\begin{aligned} \Omega''(\beta, \omega) = (\partial^2/\partial\beta^2)\Omega(\beta, \omega) = & 2(K''_{\text{eff}} - K''^* \cos \omega) \sinh(2K_{\text{eff}}^0) \cosh(2K^*) \\ & + 2(K''^* - K''_{\text{eff}} \cos \omega) \sinh(2K^*) \sinh(2K_{\text{eff}}^0) \\ & + 4(K_{\text{eff}}'^2 + K'^{*2} - 2K_{\text{eff}} K'^* \cos \omega) \cosh(2K_{\text{eff}}^0) \cosh(2K^*) \\ & + 4[2K'^* K'_{\text{eff}} - (K_{\text{eff}}'^2 + K'^{*2}) \cos \omega] \sinh(2K_{\text{eff}}^0) \sinh(2K^*) \end{aligned} \tag{52}$$

$$K'^* = \partial K^*/\partial\beta = -2J_0/\sinh(4K_0)$$

$$K''^* = \partial^2 K^*/\partial\beta^2 = 4J_0(1 + \sinh^2 2K_0)/\sinh(4K_0) \tag{53}$$

and where K_{eff}^0 , K'_{eff} and K''_{eff} are given by (36)-(38) respectively.

The integrals in (49) and (50) can be evaluated numerically and we can plot U and C/K_B against $K_B T/J_1$ for any values of α , δ and m . In figure 8 we show the specific heat for $m = 1, 2$ and 3 and for $\alpha \approx 1$ ($\delta = 1$). We note that there exist three transition temperatures ($\alpha \leq 1$), T_1 , T_2 and T_3 corresponding to the ferro \rightarrow para \rightarrow mixed \rightarrow paramagnetic transitions. As $T \rightarrow 0$, $C/K_B \rightarrow \frac{1}{4}(2n + 1)$, as happens in the one-dimensional case. In figure 8(d) we show T_1 and T_3 for $\alpha = 0.75$ ($m = 3$ case). We call the reader's attention to the scale of this latter figure. For $\alpha \rightarrow 1$ the distance between these latter peaks tends exponentially to zero, simulating a first-order transition but actually indicating that the paramagnetic phase reaches the ground state exactly at the point $T = 0$, $\alpha = 1$.

4. Infinite dimensionality limit ($m \rightarrow \infty$)

In this section we study the one-dimensional and the square lattice models for the infinite limit of the bond vector decorating spin dimensionality. In both models, the partition function and the thermodynamic functions have been obtained in the previous sections as a function of the effective exchange interaction given by (36) where the dimensionality dependence appears through the $G_n(2\lambda K_1)$ functions. In the $m \rightarrow \infty$ limit we get a very simple and close expression for the effective interaction, i.e.

$$K_{\text{eff}}^\infty = \lim_{m \rightarrow \infty} K_{\text{eff}}^0 = K_2 + K_1^2 \tag{54}$$

as shown in the appendix.

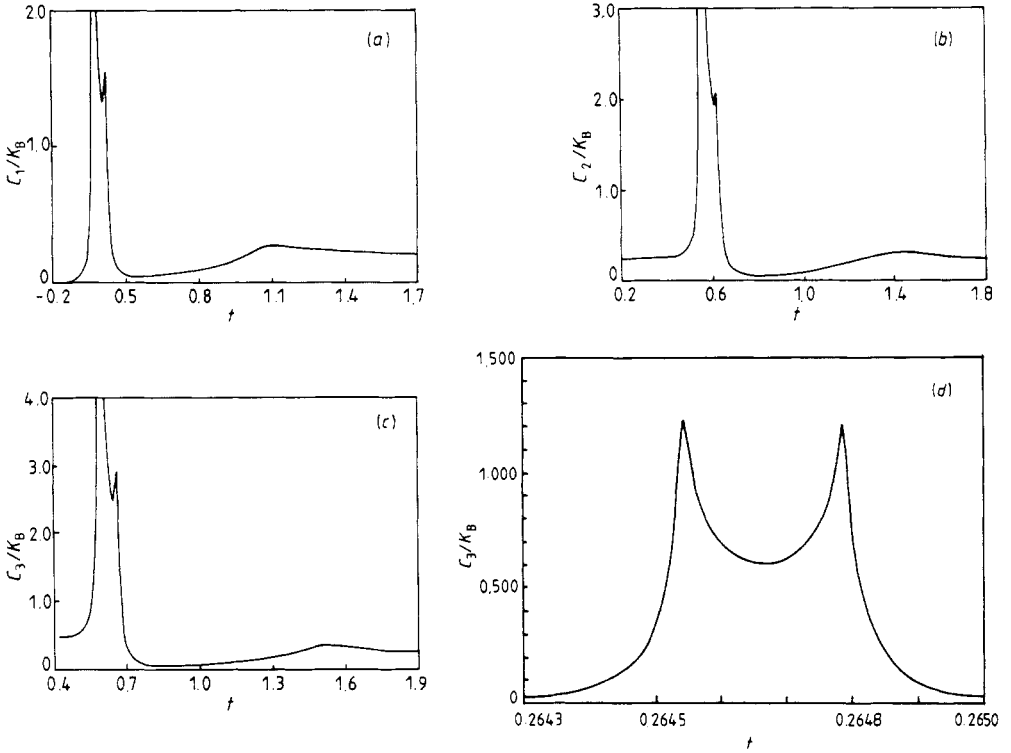


Figure 8. Specific heat C_m/K_B as a function of the reduced temperature $t = K_B T/J_1$ for (a) Ising case ($m = 1$) for $\alpha = 0.83$, (b) XY case ($m = 2$) for $\alpha = 0.655$, (c) Heisenberg case ($m = 3$) for $\alpha = 0.57$ and (d) Heisenberg case for $\alpha = 0.75$ (anisotropic 2D model).

The internal energy, the entropy and the specific heat for the one-dimensional case can be evaluated by substituting (54) in (33)–(35) respectively, resulting in

$$U_\infty = -1 - 2 \left(\frac{2}{\bar{\alpha}x} - 1 \right) \left[1 + \exp \left(\frac{2\bar{\alpha}}{x} - \frac{2}{x^2} \right) \right]^{-1} \quad (55)$$

$$\frac{S_\infty}{K_B} = \frac{1}{2} \ln \left[\exp \left(-\frac{2\bar{\alpha}}{x} + \frac{2}{x^2} \right) + 1 \right] + \left(\frac{\bar{\alpha}}{x} - \frac{2}{x^2} \right) \left[1 + \exp \left(\frac{2\bar{\alpha}}{x} - \frac{2}{x^2} \right) \right]^{-1} \quad (56)$$

$$\frac{C_\infty}{K_B} = \frac{2}{x^2} \left(1 + \frac{(2/x - \bar{\alpha})^2}{1 + \exp(2/x^2 - 2\bar{\alpha}/x)} \right) \left[1 + \exp \left(\frac{2\bar{\alpha}}{x} - \frac{2}{x^2} \right) \right]^{-1} \quad (57)$$

where $x = J_1/K_B T$ and $\bar{\alpha}$ is equal to $-J_2/J_1$. The temperature dependence behaviour of these functions is shown in figure 9 for several values of $\bar{\alpha}$. We focus our attention on the behaviour of the system close to the temperature where the effective interaction changes its signal, i.e. where the effective interaction changes from ferromagnetic to antiferromagnetic. This ‘critical’ temperature is given by $K_B T_c/J_1 = 1/\bar{\alpha}$. At this temperature there is a maximum in the specific heat that becomes sharper and higher as $\bar{\alpha}$ increases, as shown in figure 9(c) for several values of $\bar{\alpha}$.

This phase diagram $T \times \bar{\alpha}$ for the anisotropically decorated square lattice model can be obtained analytically by substituting (54) in (44) giving

$$\bar{\alpha} = K_1 \pm (1/2K_1) \ln(\coth \bar{\delta}K_1) \quad (58)$$

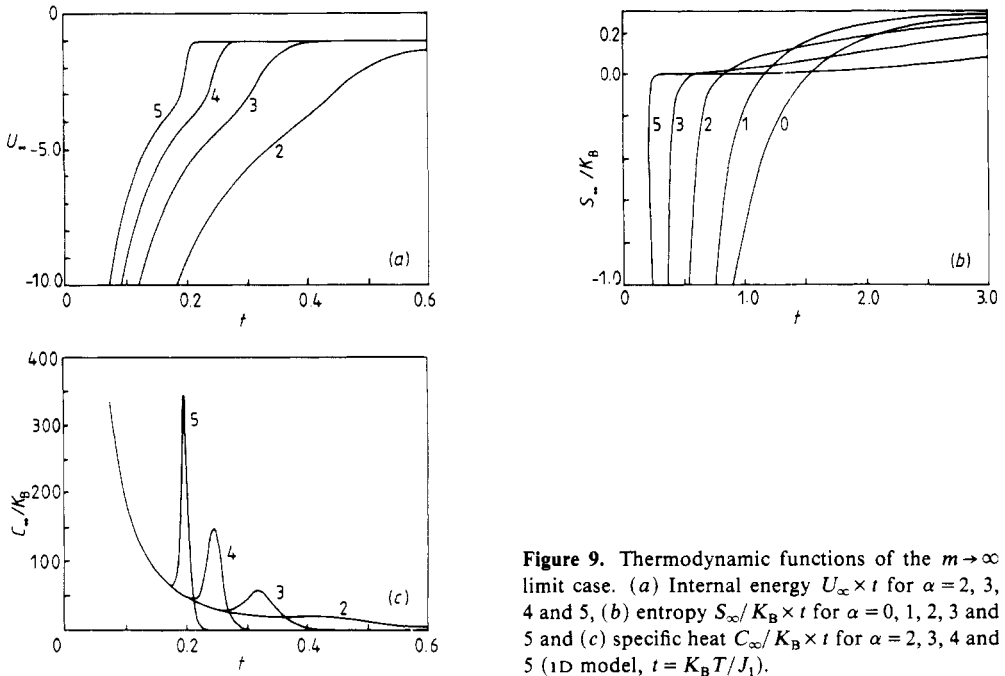


Figure 9. Thermodynamic functions of the $m \rightarrow \infty$ limit case. (a) Internal energy $U_\infty \times t$ for $\alpha = 2, 3, 4$ and 5 , (b) entropy $S_\infty / K_B \times t$ for $\alpha = 0, 1, 2, 3$ and 5 and (c) specific heat $C_\infty / K_B \times t$ for $\alpha = 2, 3, 4$ and 5 (1D model, $t = K_B T / J_1$).

where $\bar{\delta} = K_0 / K_1$. For the isotropic case, the phase diagram is given by using (44) in the equation $\sinh 2K_{\text{eff}} = \pm 1$, that is

$$\bar{\alpha} = K_1 + (1/2K_1) \ln(\sqrt{2} \pm 1). \tag{59}$$

Both diagrams are shown in figure 10. We note that the ferromagnetic phase is stable at $T = 0$ for every finite value of $\bar{\alpha}$. For the isotropic case and for $\bar{\alpha} > \alpha_c$ there are three transition temperature points, where $\alpha_c = 1.326 \dots$ is given by $K_{\text{eff}} = K_c = 0.44 \dots$. For the anisotropic case α_c can be obtained numerically by solving the transcendental equation $d\bar{\alpha} / dK_1 = 0$.

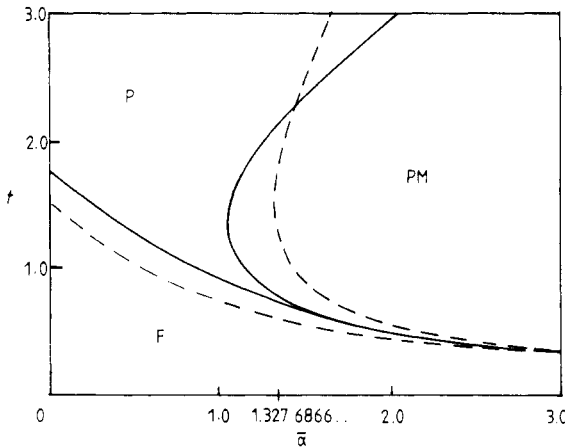


Figure 10. Phase diagram in the plane $T \times \bar{\alpha}$ for the anisotropic (—) and the isotropic (---) decorated square lattice in the $m \rightarrow \infty$ limit.

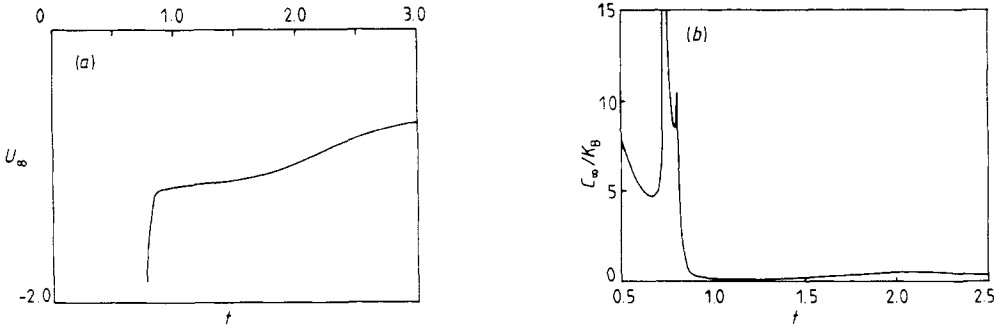


Figure 11. (a) Internal energy $U_\infty \times t$ for $\bar{\alpha} = 1.3$. (b) Specific heat $C_\infty / K_B \times t$ for $\bar{\alpha} = 1.3$ in the $m \rightarrow \infty$ limit (anisotropic 2D model).

The internal energy and the specific heat for the anisotropic case are given by (49)-(53) taking $K_{\text{eff}} = K_{\text{eff}}^\infty = K_1^2 + K_2$. In figure 11 we show the temperature behaviour of the internal energy and the specific heat for some value of $\bar{\alpha}$ in the three temperature interval and for $\bar{\delta} = 1$.

5. Summary and conclusions

We have studied the phase diagram and the thermodynamics of the one-dimensional and the square lattice Ising model decorated with m -dimensional vector spins. We have drawn attention to two aspects, namely the local frustration induced by the competing interaction between the bond vector decorating spins and the Ising spins, and the effect of the bond vector spin dimensionality on the thermodynamic properties of both models. It is well known that spin decorating is equivalent to an effective interaction that is temperature and external field dependent (Fisher 1959, Syozi 1972).

Therefore, if there is competition between the bond vector-Ising spin and the Ising spin-Ising spin interactions, the effective temperature and field dependent interaction could have its character changed from ferro- to antiferromagnetic and vice versa, as in the present model. This is evidenced by the behaviour of the pair correlation function for the one-dimensional model. At $T = 0$ the ordered phase changes with the competing parameter $\alpha = -J_2 / \sqrt{m} J_1$. For $\alpha > 1$ the Ising spins order antiferromagnetically while the bond vector remains uncorrelated and for $\alpha < 1$ all the spins, including the decorating ones, order ferromagnetically. In figure 2 we have shown that the ferromagnetic short-range order decreases monotonically with the decorating spin dimensionality for a given temperature. We note that the thermodynamic properties (internal energy, entropy and specific heat) of both models have a qualitatively distinct physical behaviour if the decorating vector spin is an Ising spin ($m = 1$ case) or a 'classical' one ($m > 1$ cases) and are strongly affected by the competing interaction, especially for $\alpha \sim 1$, due to the onset of the correlation between the decorating vector spins and the Ising spins. These features can be seen in figures 3-5 and 8-9 for the one-dimensional and square lattice models, respectively.

The phase diagram $T \times \alpha$ for the anisotropic square lattice decorated Ising model, i.e. a square lattice Ising model with decorating bond spins in one direction only, has been obtained analytically for a general dimension m . In figure 6 one can see the existence of three distinct phases meeting at the point $T = 0, \alpha = 1$, the ferro-, the para-

and the mixed or para-metamagnetic phases. In the mixed phase at $T=0$ the Ising spins are antiferromagnetically correlated while the decorating spins are uncorrelated. However as soon as the temperature becomes finite the Ising spin flip excitation will be dependent on decorating neighbouring vector spins correlation. For $\alpha < 1$ there is a three-transition temperature region characteristic of the decorated models (Syozzi 1972) that increases with the spin dimensionality. We note that the borderlines between the para-ferromagnetic phases and paramagnetic-mixed phases seems to collapse to an apparent first-order transition line. This fact is evidenced by the behaviour of the internal energy and specific heat. However one can show analytically that actually both lines meet at the point $T = 0, \alpha = 0$ as pointed out in figure 8(d).

Finally we analyse both models in the $m \rightarrow \infty$ limit. First of all we draw the reader's attention to the $m \rightarrow \infty$ limit of the effective interaction expression that has a very close and simple form, i.e. the effective interaction is just proportional to the inverse of the square temperature. For the one-dimensional system there is an abrupt change in the behaviour of the thermodynamic properties at temperatures close to the temperature where the effective interaction changes signal. There is a maximum in the specific heat that becomes sharper and higher as $\bar{\alpha} = |J_2|/J_1$ increases; see figure 9(c). For the square lattice model we get analytically the phase diagrams for both isotropic and anisotropic cases. We note that the ferromagnetic phase is stable at $T = 0$ for any finite value of $\bar{\alpha}$.

Acknowledgment

We would like to thank A F Siqueira for computational help in plotting diagrams.

Appendix. Effective exchange interaction in the $m \rightarrow \infty$ limit

The effective exchange interaction is given by (36), where $n = \frac{1}{2}m - 1$ and $\lambda = \sqrt{m}$ in order to renormalise the exchange integrals with respect to the vector spin dimensionality (Stanley 1969). We have that

$$\lim_{m \rightarrow \infty} K_{\text{eff}}^0 = K_2 + \frac{1}{2} \lim_{m \rightarrow \infty} \ln \left(\frac{2^n n!}{x^n} I_n(x) \right) \tag{A1}$$

with $x = 2\lambda K_1$. To evaluate the limit we use the expansion of the modified Bessel function of first kind (Dwight 1961)

$$I_n(x) = \sum_{p=0}^{\infty} \frac{(\frac{1}{2}x)^{n+2p}}{p! \Gamma(n+p+1)}. \tag{A2}$$

Therefore

$$\begin{aligned} K_{\text{eff}}^0|_{\infty} &= K_2 + \frac{1}{2} \lim_{m \rightarrow \infty} \ln \left(1 + \frac{(\frac{1}{2}x)^2}{1 \times (n+1)} + \frac{(\frac{1}{2}x)^4}{1 \times 2 \times (n+1)(n+2)} + \dots \right) \\ &= K_2 + \frac{1}{2} \lim_{n \rightarrow \infty} \ln \left(1 + \frac{2K_1^2}{1} + \frac{2^2(n+1)K_1^4}{1 \times 2(n+2)} + \dots \right) \\ &= K_2 + \frac{1}{2} \ln \left(1 + \frac{2K_1^2}{1} + \frac{(2K_1^2)^2}{2!} + \frac{(2K_1^2)^3}{3!} + \dots \right) \\ &= K_2 + \frac{1}{2} \ln \exp(2K_1^2) = K_2 + K_1^2 = K_{\text{eff}}^{\infty}. \end{aligned} \tag{A3}$$

References

- Dwight H B 1961 *Tables of Integrals and Other Mathematical Data* (New York: Macmillan)
- Fisher M E 1959 *Phys. Rev.* **113** 969–81
- Gonçalves L L 1982 *Physica* **110A** 339–45
- Horiguchi T and Gonçalves L L 1983 *Physica* **120A** 600–8
- Huse D A, Fisher M E and Yeomans J M 1981 *Phys. Rev. B* **23** 180–5
- McCoy B M and Wu T T 1973 *The Two-Dimensional Ising Model* (Cambridge, MA: Harvard University Press)
- Onsager L 1944 *Phys. Rev.* **65** 117
- Stanley H E 1969 *Phys. Rev.* **179** 570–7
- 1971 *Phase Transitions and Critical Phenomena* (Oxford: Clarendon)
- Syozzi I 1968 *Prog. Theor. Phys.* **39** 1367–8
- 1972 *Phase Transitions and Critical Phenomena* vol 1, ed C Domb and M S Green (New York: Academic)
pp 269–329
- Yamada I 1969 *Prog. Theor. Phys.* **42** 1106–28